

## Analytical and Semi-Analytical Tools for the Design of Oscillatory Pumping Tests

by Michael Cardiff<sup>1</sup> and Warren Barrash<sup>2</sup>

---

### Abstract

Oscillatory pumping tests—in which flow is varied in a periodic fashion—provide a method for understanding aquifer heterogeneity that is complementary to strategies such as slug testing and constant-rate pumping tests. During oscillatory testing, pressure data collected at non-pumping wells can be processed to extract metrics, such as signal amplitude and phase lag, from a time series. These metrics are robust against common sensor problems (including drift and noise) and have been shown to provide information about aquifer heterogeneity. Field implementations of oscillatory pumping tests for characterization, however, are not common and thus there are few guidelines for their design and implementation. Here, we use available analytical solutions from the literature to develop design guidelines for oscillatory pumping tests, while considering practical field constraints. We present two key analytical results for design and analysis of oscillatory pumping tests. First, we provide methods for choosing testing frequencies and flow rates which maximize the signal amplitude that can be expected at a distance from an oscillating pumping well, given design constraints such as maximum/minimum oscillator frequency and maximum volume cycled. Preliminary data from field testing helps to validate the methodology. Second, we develop a semi-analytical method for computing the sensitivity of oscillatory signals to spatially distributed aquifer flow parameters. This method can be quickly applied to understand the “sensed” extent of an aquifer at a given testing frequency. Both results can be applied given only bulk aquifer parameter estimates, and can help to optimize design of oscillatory pumping test campaigns.

---

### Introduction

To perform basic characterization of aquifer flow properties (permeability and storage coefficients), field investigators commonly implement variants of three basic strategies—constant-rate pumping tests (or, alternately, recovery tests), constant-head tests, and slug tests. Given wells at which testing and monitoring can be performed, a field practitioner faces a few decisions regarding test setup. In the case of constant-rate pumping tests, the main considerations are the design pumping flow rate, and the length of time to continue the test. With only basic knowledge of expected average aquifer properties, a reasonable choice for both of these design parameters can be deduced using standard analytical solutions. Likewise, many methods have been developed to analyze such tests across a variety of aquifer scenarios—see, for example, the recent summary by Yeh and Chang (2013). Similarly, in the case of impulse tests such as slug tests, there are a

number of recognized guidelines for designing tests to suit the particulars of a given geologic environment and well construction, and similar guidelines for applying different analytical methods (Butler 1998).

Another set of testing strategies that can be employed for formation characterization involves periodic (rather than constant) pumping strategies, in which the flow rate at a well is varied in a repeatable fashion. Several publications have noted practical and analytical benefits in applying such tests—most especially, the ease with which the resultant periodic pressure signal can be accurately extracted even in the presence of significant sensor noise and drift (Johnson et al. 1966; Kuo 1972; Hollaender et al. 2002; Rasmussen et al. 2003; Renner and Messar 2006; Bakhos et al. 2014). However, to date this strategy is not often applied in hydrogeologic characterization, and there are only a few references that offer guidance on specifics of implementation (Vela and McKinley 1970; Black and Kipp 1981). The purpose of this paper is: (1) to provide some basic test design guidance for oscillatory (or periodic) pumping tests that can be used to size field testing hardware and select operational parameters (e.g., period length and cycle magnitude); and (2) to provide a basic visual method for understanding the volume of aquifer sensed through such testing.

Several variants of what we call periodic pumping tests can be found in the literature, in which a repeated

---

<sup>1</sup>Corresponding author: Department of Geoscience, University of Wisconsin-Madison, 1412 W. Dayton St., Room 412, Madison, WI 53706; (608)-262-2361; fax: (608)-262-0693; cardiff@wisc.edu

<sup>2</sup>Department of Geosciences, Boise State University, 1910 University Drive, Boise, ID 83725-1535; (208)-426-1229; fax: (208)-426-4061; e-mail: wbarrash@boisestate.edu

Received June 2014, accepted October 2014.

© 2014, National Ground Water Association.

doi: 10.1111/gwat.12308

pumping pattern is used to cause observable pressure signals within a geologic formation. Perhaps the earliest developed example, called the pulse test in the petroleum literature, was suggested by Johnson et al. (1966) for petroleum reservoir characterization. In this test, a well is pumped at a constant rate for a set period of time, followed by a non-pumping period of time (“shut in” interval). This alternating sequence of pumping and non-pumping time intervals is repeated multiple times, and diagnostics such as the pressure transient amplitude and travel time are used to understand formation heterogeneity. In the case of the pulse test, since there is net extraction over the period of testing, the pulses appear as a periodic signal superimposed on an overall drawdown trend. Kuo (1972), in another application to petroleum exploration, suggested and analyzed the properties of sinusoidal flow tests, in which the flow rate follows a sinusoidal curve. These tests have been discussed occasionally in both the petroleum and hydrogeologic literature, appearing under several different names: cyclic flow rate tests (Rosa and Horne 1997), periodic pumping tests (Renner and Messar 2006), harmonic pumping tests (Revil et al. 2008), and oscillatory pumping tests (Cardiff et al. 2013a), among others.

While suggested over 40 years ago, there are relatively few documented field applications of periodic pumping test analyses in the hydrogeologic literature. Lavenue and de Marsily (2001) discussed an application in which sinusoidal pumping tests performed at the Waste Isolation Pilot Plant (WIPP) were used as a data source for pilot point-based inverse modeling. Rasmussen et al. (2003) applied sinusoidal pumping tests at the Savannah River site, estimating effective homogeneous aquifer parameters by using an analytical model. Renner and Messar (2006) analyzed data from a set of periodic pumping tests performed at a site in Bochum, Germany, also by using an analytical model. Maineult et al. (2008) and Revil et al. (2008) later analyzed self-potential signals associated with periodic pumping, from the same site in Germany. Becker and Gultinan (2010) applied periodic testing to a sandstone formation at the Altona Flat Rock experimental site in New York State, USA. Jazayeri Noushabadi et al. (2011) used analytical modeling of pulse pumping tests performed in the Lez aquifer of southern France to investigate the scale effects of permeability estimation. At the GEMS site in Kansas, USA, McElwee et al. (2011) used an approximate model of oscillatory pressure travel time to tomographically analyze periodic pumping test data. Most recently, Fokker et al. (2013) re-analyzed data from the periodic tests of Renner and Messar (2006) using a numerical modeling approach to estimate parameters of geometrically constrained geologic bodies.

Recent work has suggested that periodic pumping tests may provide valuable information about aquifer heterogeneity (Cardiff et al. 2013a) through tomographic (inverse) analyses. In addition, modeling of periodic tests can be performed in the frequency domain, allowing faster simulations than are possible with typical transient numerical models (e.g., Townley 1993; Cardiff et al. 2013a).

Periodic pumping tests also have several practical benefits for field implementation, especially in cases where the oscillatory pumping is “zero-mean,” that is, the pumping strategy consists of alternating periods of injection and extraction, so that no net drawdown is caused:

- Oscillating signals of known frequency are easily separated from sensor noise and drift, and from other over-printed hydrologic processes by using Fourier-domain signal processing routines (Bakhos et al. 2014).
- Zero-mean periodic pumping tests may help to avoid costs and risks associated with handling and treating significant amounts of contaminated water, relative to traditional pumping tests.
- Zero-mean periodic pumping tests of reasonable amplitudes should not cause significant contaminant plume movement, relative to traditional pumping tests, since the average flow velocity induced by such pumping is zero in all directions.
- Periodic testing can be performed at different frequencies to obtain additional information about aquifer heterogeneity (Cardiff et al. 2013a).
- In scenarios where continuous pumping is required (e.g., a pump-and-treat capture well), a periodic signal can be over-printed on the pumping well by periodically varying the pumping rate above and below the desired long-term rate.

These advantages of periodic pumping tests have been previously discussed also in the petroleum exploration literature (Hollaender et al. 2002).

A key drawback of oscillatory pumping tests, however, is that they require specialized field hardware to perform. The existing applications referenced earlier have developed a variety of methods for implementing periodic pumping tests, each with its own benefits and drawbacks. Table 1 contains a summary of methodologies and apparatuses that have been implemented in the field to generate periodic signals, along with a qualitative comparison of their limitations. Perhaps because of the large degree of variation in how periodic tests are implemented, there is almost no guidance in the literature on how to effectively implement a periodic test at a particular field site, and using a particular methodology. The purpose of this paper is to provide some broadly applicable analytical tools that can be used to assess periodic pumping feasibility and guide selection of appropriate periodic testing methodologies for field characterization.

In this work, we focus discussion on sinusoidal pumping tests of a given frequency as suggested by Kuo (1972), though theory for sinusoidal test analysis can be extended to any periodic test by using impulse and response superposition principles. In particular, we present two key results. First, we provide practical guidelines for maximizing signal propagation over a distance under physical constraints that are likely to be encountered, including limitations regarding the total volume cycled, the frequency of cycling, the maximum flow rate during cycling, and the amplitudes of pressure

**Table 1**  
**Qualitative Summary of Methods Employed to Generate Periodic Signals for Aquifer Testing in the Field, and Their Limitations**

Periodic Testing Method	Example Application	Limitation Type					Other Testing Issues
		Total Volume Cycled	High-Frequency Constraints	Low-Frequency Constraints	Maximum Flow Rate During Cycle	Pumping Well Pressure Changes	
Pulsed extraction	Jazayeri Noushabadi et al. (2011)		Important		Very important	Important	Oscillatory flow superposed on overall drawdown signal
Sinusoidal pumping rate variation	Lavenue and de Marsily (2001)		Important		Very important	Important	Oscillatory flow superposed on overall drawdown signal
Sinusoidal injection/extraction from surface tank	Rasmussen et al. (2003)	Very important	Important		Very important	Important	
Sinusoidal raising/lowering of a solid slug	Becker and Guiltinan (2010)	Very important	Important	Important			Flow rates to formation may be impacted by well hydraulics
Sinusoidal movement of in-borehole piston	BHRS (this work)	Very important	Important	Important		Important	
Sinusoidal variation of air pressure above water column	PneuSine testing <sup>1</sup>	Very important	Important				Total volume that can be cycled dependent on unscreened interval available

<sup>1</sup>Further information on PneuSine testing can be found at: [http://www.in-situ.com/cp/uploads/PneuSine\\_Test\\_HydroResolutionsLLC.pdf](http://www.in-situ.com/cp/uploads/PneuSine_Test_HydroResolutionsLLC.pdf).

changes generated near the oscillating pumping well. This set of guidelines is validated through observed signal amplitudes from a set of oscillatory pumping tests performed at the Boise Hydrogeophysical Research Site (BHRS). Second, we present a method for quickly visualizing and understanding the sensitivity of oscillatory tests to spatially distributed aquifer flow parameters (i.e., heterogeneity). These two tools provide quick methods for evaluating the feasibility of sinusoidal testing for particular sites, for developing appropriate sinusoidal testing experimental designs, and for understanding the impact of heterogeneity on oscillatory pumping test responses.

### Mathematical Formulation

We consider periodic testing in which the linear approximation of periodic flow applies throughout the aquifer (for a relevant discussion of the range of applicability of this approximation, see Smith 2008), and thus one of the following governing equations can be used. For a two-dimensional (2D) aquifer test (i.e., fully penetrating), the following governing equation is assumed within the aquifer:

$$S(\mathbf{x}) \frac{\partial h}{\partial t} = \nabla \cdot (T(\mathbf{x}) \nabla h) \quad (1)$$

where  $\mathbf{x}$  represents the spatial coordinates vector,  $t$  represents time, and  $S$  [-] and  $T$  [ $L^2/T$ ] are the 2D aquifer flow parameters storativity and transmissivity (both assumed to be time invariant).

Likewise, for a three-dimensional (3D) aquifer test (e.g., a partially penetrating test over a small testing interval), the following governing equation is assumed within the aquifer:

$$S_s(\mathbf{x}) \frac{\partial h}{\partial t} = \nabla \cdot (K(\mathbf{x}) \nabla h) \quad (2)$$

where specific storage  $S_s$  [ $L^{-1}$ ] and hydraulic conductivity  $K$  [ $L/T$ ] (assumed isotropic at the scale of interest) are flow parameters for an aquifer experiencing 3D flow. In both cases,  $h$  [ $L$ ] is the hydraulic head field variable, which varies with space and time.

In the case where a periodic test consists of sinusoidal pumping at a point location with a single, known frequency, the source term is considered as a point source located at the origin, with a time-varying flow rate equal to:

$$Q(t) = Q_{\text{peak}} \cos(\omega t) \quad (3)$$

where  $Q_{\text{peak}}$  is a peak volume flow rate [ $L^3/T$ ], and  $\omega$  [ $1/T$ ] is the angular frequency, equal to  $2\pi/P$ , where  $P$  [ $T$ ] is the pumping period. If the aquifer is assumed to

be homogeneous and infinite in extent, and if pumping is represented as a point source in either 2D or 3D, radially symmetric analytical solutions can be derived that satisfy these governing equations. Furthermore, the problem can be simplified by only modeling the “steady-periodic” conditions, represented by consistent amplitude and phase at every point in space, which occurs once the oscillatory flow field has developed (often after about 1 to 5 periods of oscillation). Once steady periodic conditions are achieved, head change in the aquifer can be represented as:

$$h'(r, t) = \text{Re} [\Phi(r) \exp(i\omega t)] \quad (4)$$

where  $r$  [L] represents radial distance from the sinusoidal pumping well,  $\text{Re}$  represents the real part of the given argument, and  $\Phi$ , the wave phasor, is a complex variable that determines the amplitude and phase of the head changes at every point in space. Black and Kipp (1981) originally derived the analytical solutions for the phasor under both 2D (line source) and 3D (point source) cases. In the 2D (line source) case, the solution is:

$$\Phi(r) = \frac{Q_{\text{peak}}}{2\pi T} K_o \left( \left( \frac{\omega r^2 S}{T} \right)^{1/2} \exp(i\pi/4) \right) \quad (5)$$

where  $K_o$  is the modified Bessel function of the second kind. For the 3D (point source) case,

$$\Phi(r) = \frac{Q_{\text{peak}}}{4\pi K r} \exp \left( - \left( \frac{1+i}{2^{1/2}} \right) \left( \frac{\omega S_s r^2}{K} \right)^{1/2} \right) \quad (6)$$

## Optimization Formulation for Test Design

A successful periodic test can be considered one in which (1) the field hardware is able to reliably generate a periodic flux “source” with desired parameters; and (2) the signal is measurable at an observation (“receiver”) well, such that it can be processed and information can be extracted. The source of stimulation, in field practice, is always bounded by technical limitations. Technical constraints affecting source properties are summarized qualitatively in Table 1, which shows testing methods that have been used to cause periodic pressure changes in a formation. In general, testing strategies that make use of pumps will face limitations on maximum attainable flow rates, and on the ability to produce high-frequency signals. Conversely, strategies that rely on pistons or slugs are inherently limited by the total volume cycled per period.

Consider that an oscillatory testing apparatus is developed that can be operated to obtain a variety of different flow rates and periods, all of the form:

$$Q(t) = Q_{\text{peak}} \cos \left( \frac{2\pi t}{P} \right) \quad (7)$$

The design parameters for the oscillating pumping test are  $P$  and  $Q_{\text{peak}}$ . Note that, for a chosen period and

peak flow rate, the total volume injected/extracted per half period is:

$$V = \int_{-P/4}^{P/4} Q_{\text{peak}} \cos(2\pi t/P) dt = Q_{\text{peak}} P/\pi \quad (8)$$

To determine whether sinusoidal testing is feasible at a given site, one should verify in advance that one can expect to clearly observe responses at wells separated by a given radial spacing from the oscillating pumping well. However, the propagation distance of signals is crucially dependent on the period of the sinusoidal signal and the peak volume flow rate, both of which may be modified. To determine overall feasibility of testing, we formulate an optimization problem in which one seeks to maximize the signal magnitude at a given radius from the pumping well subject to relevant design constraints:

$$\max_{P, Q_{\text{peak}}} M(r_{\text{obs}}, Q_{\text{peak}}, P) \quad (9)$$

subject to:

$$0 \leq Q_{\text{peak}} \leq Q_{\text{max}} \quad (10)$$

$$P_{\text{min}} \leq P \leq P_{\text{max}} \quad (11)$$

$$0 \leq V \leq V_{\text{max}} \quad (12)$$

$$M(r_{\text{pump}}, Q_{\text{peak}}, P) \leq M_{\text{pump}} \quad (13)$$

where  $M(r_{\text{obs}}, Q_{\text{peak}}, P)$  is a function that calculates the amplitude of head oscillations at a distance from the origin, and the constraints represent, respectively: maximum peak flow rates obtainable, minimum and maximum oscillation periods obtainable, maximum total volume cycled during oscillation, and maximum head changes allowed at the radius of the oscillating well casing  $r_{\text{pump}}$ . If the maximum signal amplitude found through such an optimization is easily measurable, then it is likely that the well arrangement and the aquifer are amenable to testing with oscillating signals at a range of periods. However, if the maximum signal amplitude found through this optimization is expected to be very weak, there is little hope of obtaining any meaningful data with the provided equipment limitations and well-field design.

## Optimization Under Volume Constraints Alone

We consider first the simple case in which the only relevant constraint is the total cycle volume of the oscillating signal generator (OSG). Referring back to Equation 4, the amplitude of a response at a given location can be found as the modulus (amplitude) of the phasor, i.e.

$$M = |\Phi| = \left( \text{Re}(\Phi)^2 + \text{Im}(\Phi)^2 \right)^{1/2} \quad (14)$$

### Point-Source Case

If the total volume of an oscillator is limited by  $V_{\max}$ , then Equation 8 above implies that, for any given period, the maximum flow rate obtainable will be:

$$Q_{\text{peak}} = \frac{V_{\max}\pi}{P} \quad (15)$$

This maximum flow rate will lead to the maximum possible signal at a given period  $P$ , subject to the total volume constraint. The magnitude of the response at any point in space can be written by taking the modulus of Equation 6 and substituting in Equation 15:

$$M_{\text{ptsrc}} = \frac{V_{\max}}{4PKr_{\text{obs}}} \exp \left[ -r_{\text{obs}} \left( \frac{\pi S_s}{PK} \right)^{1/2} \right] \quad (16)$$

We seek to maximize the amplitude at a given distance (and for given approximate estimates of  $K$  and  $S_s$ ). Taking the usual approach of differentiating and setting derivatives equal to 0, we find:

$$\begin{aligned} \frac{\partial M_{\text{ptsrc}}}{\partial P} &= \frac{\partial}{\partial P} \left[ \frac{V_{\max}}{4PKr_{\text{obs}}} \exp \left[ -r_{\text{obs}} \left( \frac{\pi S_s}{PK} \right)^{1/2} \right] \right] \\ &= \left( -\frac{V_{\max}}{4P^2Kr_{\text{obs}}} + \frac{V_{\max}\pi^{1/2}S_s^{1/2}}{8K^{3/2}P^{5/2}} \right) \exp \left[ -r_{\text{obs}} \left( \frac{\pi S_s}{PK} \right)^{1/2} \right] \end{aligned}$$

Since the exponential term will never be 0 unless  $P \rightarrow 0$  (which would imply a non-physical infinite-frequency oscillator), we set the first term to 0 and find:

$$P = \frac{\pi S_s r_{\text{obs}}^2}{4K} \quad (17)$$

So, for an oscillator setup with total cycle volume constraint  $V_{\max}$  on the oscillator, and where we are trying to obtain the largest measurable signal at distance  $r_{\text{obs}}$ , the optimum period  $\hat{P}$  and flow rate amplitude  $\hat{Q}_{\text{peak}}$  are:

$$\hat{P} = \frac{\pi S_s r_{\text{obs}}^2}{4K} \quad (18)$$

$$\hat{Q}_{\text{peak}} = \frac{4V_{\max}K}{S_s r_{\text{obs}}^2} \quad (19)$$

At this distance, the signal amplitude expected using period  $\hat{P}$  can be found by plugging Equation 18 into Equation 16, yielding:

$$\hat{M}_{\text{ptsrc}} = \frac{V_{\max}}{\pi S_s r_{\text{obs}}^3} \exp(-2) \quad (20)$$

where  $\hat{M}_{\text{ptsrc}}$  is the maximum possible signal amplitude attainable at distance  $r_{\text{obs}}$  under volume constraints.

Equation 20 provides a guideline for oscillator system sizing which is notably independent of aquifer hydraulic conductivity. As a relatively general example, supposing a

representative (confined storage)  $S_s$  value of  $\approx 10^{-6}$  (1/m), and likewise supposing that signals obtained must be on the order of 1 mm in order to be measurable, this implies that, under confined conditions, the volume required to generate a measurable signal scales with distance to be investigated as:

$$V \approx r_{\text{obs}}^3 \times 2.32\text{E} - 8$$

### Line-Source Case

For the case of a fully penetrating sinusoidal pumping well, the analogous signal amplitude is obtained from plugging Equation 15 into the 2D phasor solution, Equation 5, and taking the modulus, as before. The obtained amplitude is:

$$\begin{aligned} M_{\text{linesrc}} &= |C| = (Re(C)^2 + Im(C)^2)^{1/2} \\ C &= \frac{V_{\max}}{2PT} K_0 \left[ \left( \frac{2\pi r_{\text{obs}}^2 S}{PT} \right)^{1/2} \exp(i\pi/4) \right] \end{aligned} \quad (21)$$

Multiplying the amplitude  $M_{\text{linesrc}}$  [L] by  $r^2 S/V_{\max}$  [1/L], we obtain a non-dimensional amplitude that we denote  $\mu$ :

$$\begin{aligned} \mu &= \frac{M_{\text{linesrc}} r_{\text{obs}}^2 S}{V_{\max}} \\ &= \left| \frac{\lambda}{4\pi} K_0 [\lambda^{1/2} \exp(i\pi/4)] \right| \end{aligned} \quad (22)$$

where  $\lambda$  is the dimensionless quantity  $2\pi r_{\text{obs}}^2 S/PT$ . The value of  $\lambda$  which maximizes the non-dimensional amplitude  $\mu$  (denoted  $\hat{\lambda}$  and  $\hat{\mu}$ , respectively), can be found through numerical optimization, and is:

$$\hat{\lambda} \approx 4.7183 \quad (23)$$

$$\hat{\mu} = \mu(\hat{\lambda}) \approx 0.0661$$

Thus, for a constant-volume fully penetrating oscillator system, the optimal period  $\hat{P}$  and associated flow rate amplitude  $\hat{Q}_{\text{peak}}$  are:

$$\hat{P} = \frac{2\pi r_{\text{obs}}^2 S}{\hat{\lambda} T} \approx \frac{2\pi r_{\text{obs}}^2 S}{4.7183 T} \quad (24)$$

$$\hat{Q}_{\text{peak}} = \frac{V_{\max} \hat{\lambda} T}{2r_{\text{obs}}^2 S} \approx \frac{4.7183 V_{\max} T}{2r_{\text{obs}}^2 S} \quad (25)$$

At this optimal period, the signal amplitude obtained is maximized and is equal to:

$$\hat{M}_{\text{linesrc}} = \frac{\mu(\hat{\lambda}) V_{\max}}{r_{\text{obs}}^2 S} \approx 0.0661 \frac{V_{\max}}{r_{\text{obs}}^2 S} \quad (26)$$

## Optimization Under Multiple Constraints

The key formulas presented above (Equations 18–20 and Equations 24–26) provide analytical results that can quickly be used in the field with simple computations that require only a calculator. The more general optimization formulation, Equations 9–13, which includes constraints on the maximum and minimum period, maximum and minimum allowable flow rates, and maximum near-well head change, is a nonlinearly constrained optimization problem with a nonlinear objective function—generally a quite difficult problem. It turns out, however, that the more general formulation can be solved semi-analytically due to some nice mathematical properties. Specifically, the objective function is provably monotonic within the feasible region of the optimization problem, and thus the optimum period and flow rate must fall along one of the constraint boundaries. For the reader interested in the mathematical details of this derivation, we provide them in Appendix S1, Supporting Information, for this paper. For the purposes of this paper, we simply provide the final analytical result, along with MATLAB code that can be used to perform the computations.

### Point-Source Case

For the point-source case, the following steps should be performed in order to find the  $P$  and  $Q_{\text{peak}}$  that correspond to the optimum signal propagation:

- 1 Check whether the point  $P = \pi S_s r_{\text{obs}}^2 / 4K$ ,  $Q_{\text{peak}} = 4V_{\text{max}} K / S_s r_{\text{obs}}^2$  meets all of the problem constraints. If so, evaluate  $M_{\text{ptsrc}}$  at this location.
- 2 Evaluate  $M_{\text{ptsrc}}$  at all other intersection points of constraint equalities that define the boundaries of the feasible region.
- 3 The global optimum must be, amongst those points found in Steps 1 and 2, the point with the highest  $M_{\text{ptsrc}}$  value.

This algorithm is implemented in the supplied MATLAB code `oscill_opt_ptsrc_nonlcon.m`.

To test these algorithms, we show optimizations for three different hypothetical aquifer testing scenarios. All three scenarios (with parameters given in Table 2) represent confined aquifers, though they span a range of hydraulic conductivity values. In each case, we assumed a relatively small volume of oscillation (less than 10L), and a relatively small well spacing of 10 to 20m, appropriate perhaps for detailed contaminated site investigation. While appropriate for some types of hydrogeologic investigations, other cases (e.g., with larger cycle volumes and larger inter-well distances) can be tested using the supplied code. Figure 1 shows several examples of the feasible region and objective function value for the three different cases, and this figure emphasizes that the location of the global optimum is dependent on the particular scenario under study. In all cases, the small circle represents the location of the optimum found by applying the above algorithm. As can

**Table 2**  
Parameters Used in the Optimization Test Cases Shown in Figure 1

	Case (a)	Case (b)	Case (c)
<i>Inputs</i>			
$K$ (m/s)	1E-03	1E-06	1E-07
$S_s$ (1/m)	1E-06	1E-06	1E-06
$r_{\text{obs}}$ (m)	10	20	20
$V_{\text{max}}$ (L)	10.0	0.2	1.0
$P_{\text{max}}$ (s)	3600	3600	10,000
$P_{\text{min}}$ (s)	10	50	100
$r_{\text{pump}}$ (m)	0.05	0.10	0.10
$M_{\text{pump}}$ (m)	1.00	2.00	1.00
<i>Optimized testing parameters</i>			
$P$ (s)	49.98	314.16	10,000
$Q_{\text{peak}}$ (L/s)	6.29E-01	2.00E-03	1.26E-04
$M$ (mm)	4.62	1.08	1.64

be seen, the algorithm locates the optimum period and peak flow rate for obtaining a maximum signal amplitude.

### Line-Source Case

The algorithm for the line-source (fully penetrating) case is only slightly different:

- 1 Check whether the point  $P = 2\pi r_{\text{obs}}^2 S / \hat{\lambda} T$ ,  $Q_{\text{peak}} = \hat{\lambda} T V_{\text{max}} / 2r_{\text{obs}}^2 S$  meets all of the problem constraints. If so, evaluate  $M_{\text{linesrc}}$  at this location.
- 2 Evaluate  $M_{\text{linesrc}}$  at all other intersection points of constraint equalities that define the boundaries of the feasible region.
- 3 The global optimum must be, amongst those points found in Steps 1 and 2, the point with the highest  $M_{\text{linesrc}}$  value.

This algorithm is implemented in the supplied MATLAB code `oscill_opt_linesrc_nonlcon.m`.

### Field Data Example

A set of partially penetrating (1 m interval) oscillatory pumping test experiments were planned and carried out during Summer, 2013, at the Boise Hydrogeophysical Research Site (BHRS) as a preliminary effort to validate the use of oscillatory pumping for aquifer imaging (Cardiff et al. 2012b). The aquifer at the BHRS consists of sand-and-gravel deposits adjacent to the Boise River, with an average  $K \approx 8e-4$  [m/s] (Barrash et al. 2006). The aquifer is unconfined with an average porosity of  $\approx 0.22$  [-] (Barrash and Clemon 2002), though prior testing at the site analyzing pumping tests of 20 to 1000 min in duration have obtained “effective” (i.e., partially drained) specific yield values of  $S_y \approx 0.03$  [-] (Barrash et al. 2006). Specific storage has been estimated previously at around  $S_s \approx 4e-5$  [1/m], using standard constant-rate pumping tests analyzed with homogeneous models (Barrash et al. 2006). Primary infrastructure at the site consist of 18 fully

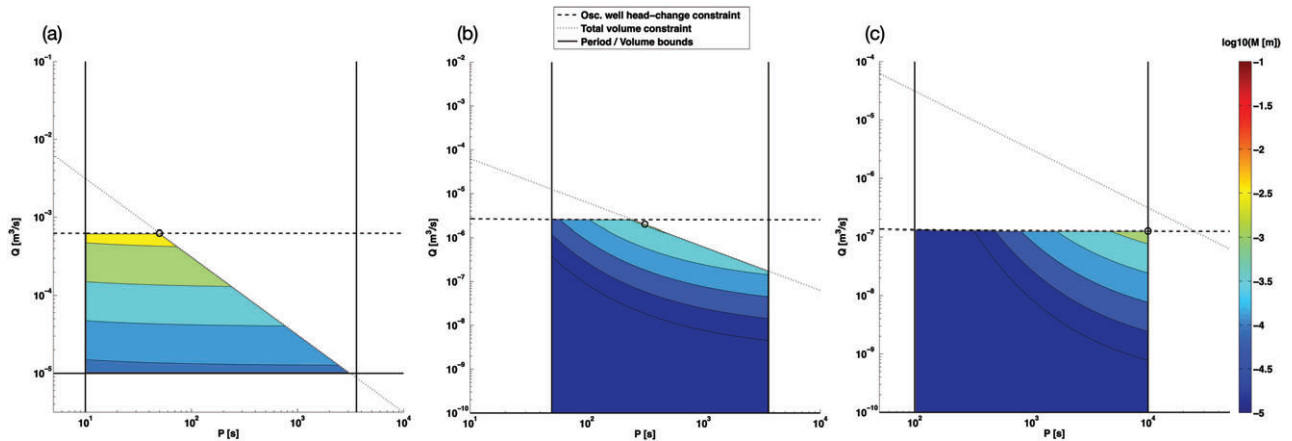


**Figure 1.** Three examples of constrained optimization of oscillatory pumping. Colored area shows objective function value (signal magnitude), with lines representing implemented constraints. The circle in each case represents the optimal parameter set chosen, based on the supplied MATLAB code. Visual inspection of the full objective function plot shows that the optimum found is the location of the largest feasible signal magnitude. Note that in each case a different set of optimization constraints is active (i.e., the optimum does not always fall along the same constraint boundary).

penetrating wells screened throughout the sand-and-gravel formation and completed into an underlying aquitard. The central well field consists of a central well (A1) surrounded by two roughly concentric “rings” of six wells each (B1 to B6 wells and C1 to C6 wells). Lastly a set of five wells (X1 to X5) surround the central well field and provide the ability to monitor boundary condition impacts. Other wells, piezometers, and monitoring instrumentation have been installed at the site throughout its history, and numerous characterization efforts have been performed including hydrologic and geophysical methods. A full summary of site activities is beyond the scope of the text, though the interested reader is directed to our prior publications that describe site design and testing results (Barrash et al. 1999, 2006; Barrash and Clemo 2002; Cardiff et al. 2009, 2011, 2012a, 2013b), as well as to the site webpage at <http://cgiss.boisestate.edu/bhrs/>.

An oscillating in-well “piston” design was developed in which a metal shaft with maximum stroke length 0.91 m (for a total displacement of  $\approx 1.85$  L) would be used to cause injection and extraction of water from the desired testing interval without removing water from the well or pumping water into the well from the surface. A piston at the land surface was moved by an electric motor connected to a crankshaft which converted rotational energy to reciprocal motion. The surface piston was then hydraulically connected to a sealed, down-hole piston below the water table which acted on a 1-m aquifer interval, sealed above and below with packers. This down-hole piston thus directly forced water into the formation at the given testing interval during downward piston movement and pulled water out of the formation during upward piston movement. Based on the engine used and gearing, it was estimated that the OSG would be able to produce oscillation periods between roughly 1 and 100 s.

Before performing field experiments, we utilized the developed equations to determine the feasibility of oscillatory pumping tests based on the above design

constraints. Because the pumping tests planned would perform oscillations within a small interval in the aquifer, we chose to use the point-source set of formulas as an approximation to predict responses. The Black and Kipp (1981) formulas, as noted earlier, assume an aquifer under confined conditions with infinite extent in all three directions. This is a very rough approximation of the BHRs aquifer, which has a saturated thickness of about 16.5 m during the Summer testing period. In order to apply the developed formulas, a single representative value for aquifer storage must also be chosen. This again requires a rough approximation of the BHRs aquifer that experiences both compressive storage and water table (drainable) storage. Based on prior experience, the representative storage value was chosen to be equal to the specific storage coefficient of  $4e - 5$  [1/m]. This approximation was deemed reasonable based on observations of the amount of time required (10 min or more) to achieve representative “late time” storage behavior during constant-rate pumping tests (Barrash et al. 2006), though it should be noted that this approximation can be expected to be less accurate when pumping takes place near the water table. A measurement radius of 15 m between oscillating pumping and observation locations was chosen, representing some of the larger distances expected from the test design.

Using the parameters above, the simpler formulation considering only volume constraints (Equations 18–20) yields:  $\hat{P} \approx 9$  s,  $\hat{Q}_{\text{peak}} \approx 0.65$  L/s, and  $\hat{M} \approx 0.6$  mm. Notably, this period of oscillation was well within the range expected to be possible with the planned OSG, and a head-change magnitude of 0.6 mm (or 1.2-mm peak-to-trough amplitude) was known to be measurable with the fiber-optic pressure sensors planned for use. The additional constraint of ensuring reasonable drawdowns/pressure build-ups near the pumping well is important at the BHRs aquifer, so we additionally applied the constrained optimization in which the casing radius

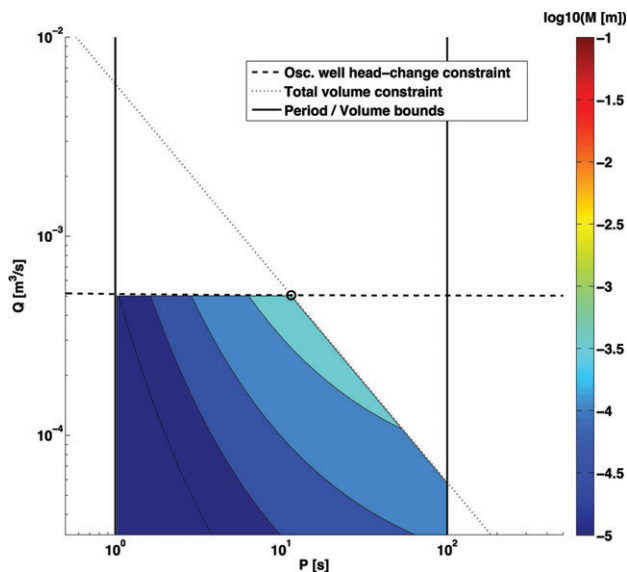


**Figure 2.** Results of optimization of field testing plan for the BHRS. Circle shows optimal value obtained by application of formulas. Colored area shows feasible region for this application, showing a range of periods across which signals of 1 mm or greater are expected to be detectable.

of the pumping well,  $r_{\text{well}}$ , was set to 0.05 m, and the maximum head change allowed at the casing radius was  $M_{\text{pump}} = 1$  m. Cycle periods of 1–100 s were used as constraints for the period. The results of the constrained optimization are shown in Figure 2, where an optimum period of  $\hat{P} \approx 11.5$  s is obtained. The optimum being at this slightly longer pumping period is due to the near-well head-change constraint (i.e., formula 13), but does not result in a significant change in the optimum signal magnitude ( $\hat{M} = 0.58$  mm). The gentle decrease in the objective function in Figure 2 also shows that there is a fairly broad range of periods across which oscillating testing is expected to yield measurable signals at a distance of 15 m.

Field testing was carried out during July 2013 using the piston OSG described earlier. Examples of raw observation data obtained from the BHRS testing are shown on the left in Figure 3, for four different oscillation periods. In each of these tests, oscillations were induced in a 1-m interval in a testing well (B3), with the interval centered at roughly 5 m below the water table. The responses shown represent pressure changes in a well located 10.55 m away laterally (C4), in a 1-m observation interval centered 10.6 m below the water table. Given the site geometry, the data here represent head-change signals collected by a transducer located 11.83 m total distance from the oscillating pumping location. Coherent signals in the raw data demonstrate that even small-volume oscillations ( $\approx 0.45L$  was used in this case) are measurable over distances of  $\approx 12$  m. The frequency spectra for these signals (Figure 3, right) show that power on the order of 0.4 to 0.7 mm head change is observed for tests at periods of 8 to 25 s with the highest peaks occurring when the pumping period is around 14 s (Figure 3c). It should be noted that secondary peaks

can be found in many of these frequency spectra, and represent harmonics of the fundamental testing frequency. This is due to the fact that the oscillatory testing apparatus produced a periodic but not exactly sinusoidal stimulation. Similarly to the results predicted by the pre-test analyses (Figure 2), high signal powers are produced even at longer stimulation periods than the predicted 9- to 12-s optimum, though they decrease somewhat at longer periods (Figure 3a and 3b) and appear to rapidly attenuate at shorter periods (Figure 3d).

## Sensitivity Analysis

Steady-periodic theory can be used to derive sensitivity maps that show the sensitivity of measurements to parameters such as spatially distributed  $K$  and  $S_s$ . These analyses show that measurements, such as signal amplitude and phase recorded at an observation well, have different averaging volumes associated with different testing periods. Perhaps unsurprisingly, tests at short periods (high frequencies) are more dependent on near-field aquifer heterogeneities, whereas longer period (lower frequency) tests are sensitive to aquifer heterogeneities over a larger volume.

One method for investigating the “averaging volume” associated with aquifer testing is through adjoint sensitivity analyses (see, e.g., formulations in Sykes et al. 1985; Neupauer and Wilson 1999; Cirpka and Kitanidis 2001; Cardiff and Kitanidis 2008), which provide mathematical expressions for computing the sensitivity of an observation to spatially distributed aquifer properties. The most common use of adjoint sensitivity calculations is in the numerical computation of spatial sensitivities required during tomographic inverse problems. However, adjoint sensitivity integrals can also be combined with analytical (homogeneous) solutions. Sensitivity maps derived in this way represent the linearized sensitivity of an observation to perturbations in aquifer parameters throughout the domain. As an example, Leven and Dietrich (2006) present an analysis showing how the Theis solution can be combined with adjoint state theory to understand the sensitivity of constant-rate pumping test observations to spatially distributed aquifer heterogeneity. In this section, we present a similar analysis for the case of oscillating flow tests at different frequencies. We first review the key formulas used to compute adjoint state sensitivities for oscillatory flow problems and then show how analytical solutions can be used to develop sensitivity maps quickly. These maps provide a visual explanation of the changes in the sensed region of an aquifer under different pumping frequencies, and can be used to assess what portion of an aquifer is being interrogated by a given testing design (i.e., the well locations and oscillatory period).

## Adjoint Theory

As developed in Cardiff et al. (2013a), for an infinite domain  $\Omega$ , the sensitivity of a measurement  $m_i$  to a

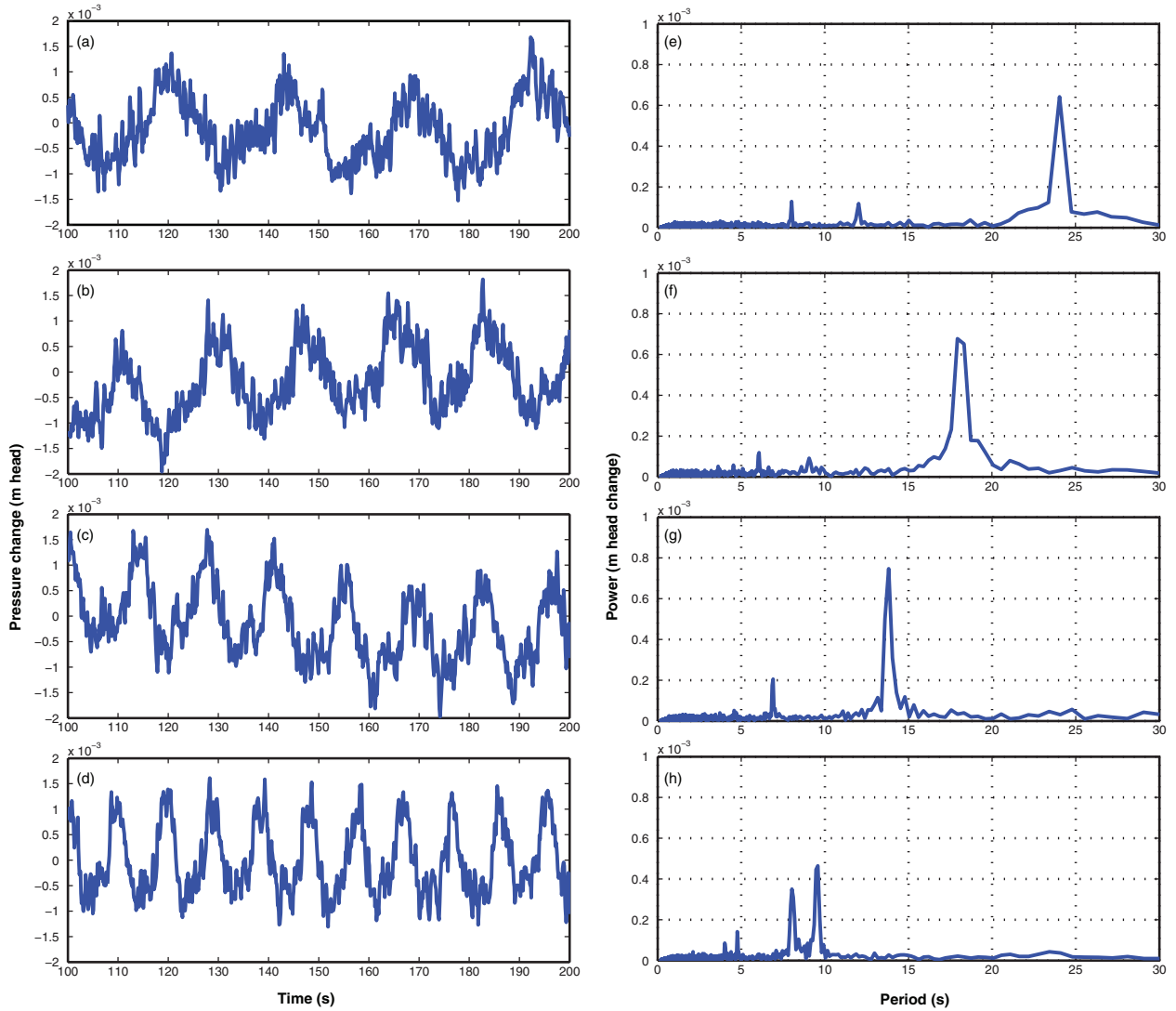


**Figure 3. Field data from the BHRS 2013 testing campaign. 100 s of raw data at four different periods (left), and frequency spectra (right) showing strong peaks at the testing frequency and associated harmonics.**

parameter value  $p$  is found using the adjoint state formulation as:

$$\frac{\partial m_i}{\partial p} = \int_{\Omega} i\omega\psi_i \frac{\partial S_s}{\partial p} \Phi_{\omega} + \frac{\partial K}{\partial p} \nabla \Phi_{\omega} \cdot \nabla \psi_i d\Omega, \quad (27)$$

where  $\omega$  is the angular frequency of the testing,  $\Phi_{\omega}$  is the phasor solution at that frequency, and  $K$  and  $S_s$  represent assumed average conductivity and storage parameters for an aquifer. The variable  $\psi_i$  is the so-called “adjoint field variable,” which is used in sensitivity calculation. For the case of a point observation, the adjoint field solution is found by solving the steady-periodic flow problem with an appropriate point-source term located at the observation point.

In particular, an intuitive set of signal metrics describing response at an observation point are the amplitude and phase offset of the measured signal (with phase measured relative to the source signal). As shown in the appendix of Cardiff et al. (2013a), this can be represented by defining a complex-valued observation

$m_i$  that contains the log-amplitude and phase (i.e., the complex modulus and complex argument) as its real and imaginary components:

$$m_i = \int_{\Omega} r_i d\Omega \quad (28)$$

$$r_i = [\ln(|\Phi_{\omega}|) + i \arg(\Phi_{\omega})] \delta(\mathbf{x} - \mathbf{x}_i) \quad (29)$$

where  $\mathbf{x}_i$  is the location of measurement  $i$ . The mathematical details and background for this choice are beyond the scope of this work, but can be found in the reference given above. The key result, however, is that the adjoint source term for such an observation should be equal to:

$$\frac{\partial r_i}{\partial \Phi_{\omega}} = \frac{1}{\Phi_{\omega}} \delta(\mathbf{x} - \mathbf{x}_i) \quad (30)$$

that is, a point source with magnitude  $1/\Phi_{\omega}$ .

We now combine the adjoint state equations above with the analytical solutions developed by Black and

Kipp (1981) for point-source and line-source solutions. This makes it possible to generate sensitivity maps that can be used to understand the averaging volumes associated with testing at different periods. The key steps to performing such an analysis are outlined below, and an implementation of this process can be found in the supplied MATLAB codes `oscill_sens_linesrc_vis.m` and `oscill_sens_ptsrc_vis.m`, along with their associated called functions.

1 Supply the location of the oscillating pumping well, the maximum flow rate  $Q_{\text{peak}}$ , the angular frequency of oscillation  $\omega$ , the location of the observation well, and approximate estimates of the aquifer conductivity and storage parameters.

- 2 The phasor-domain solution,  $\Phi_\omega$ , is given by the appropriate 2D or 3D (Black and Kipp 1981) solution.
- 3 Calculate the phasor value of the Black and Kipp (1981) solution at the location of the observation well, and call this  $\Phi_{\text{obs}}$ .
- 4 The adjoint solution,  $\psi_i$ , is given by the appropriate 2D or 3D Black and Kipp (1981) solution with  $Q_{\text{peak}}$  set equal to  $1/\Phi_{\text{obs}}$ .
- 5 Based on Equation 27, the sensitivity map of signal log-magnitude or phase to conductivity or storage parameters can be found through the appropriate inner product:

- Sensitivity of log-amplitude,  $\ln(|\Phi_\omega|)$ , to  $\ln(K)$ :  $Re(K \nabla \Phi_\omega \cdot \nabla \psi_i)$ .

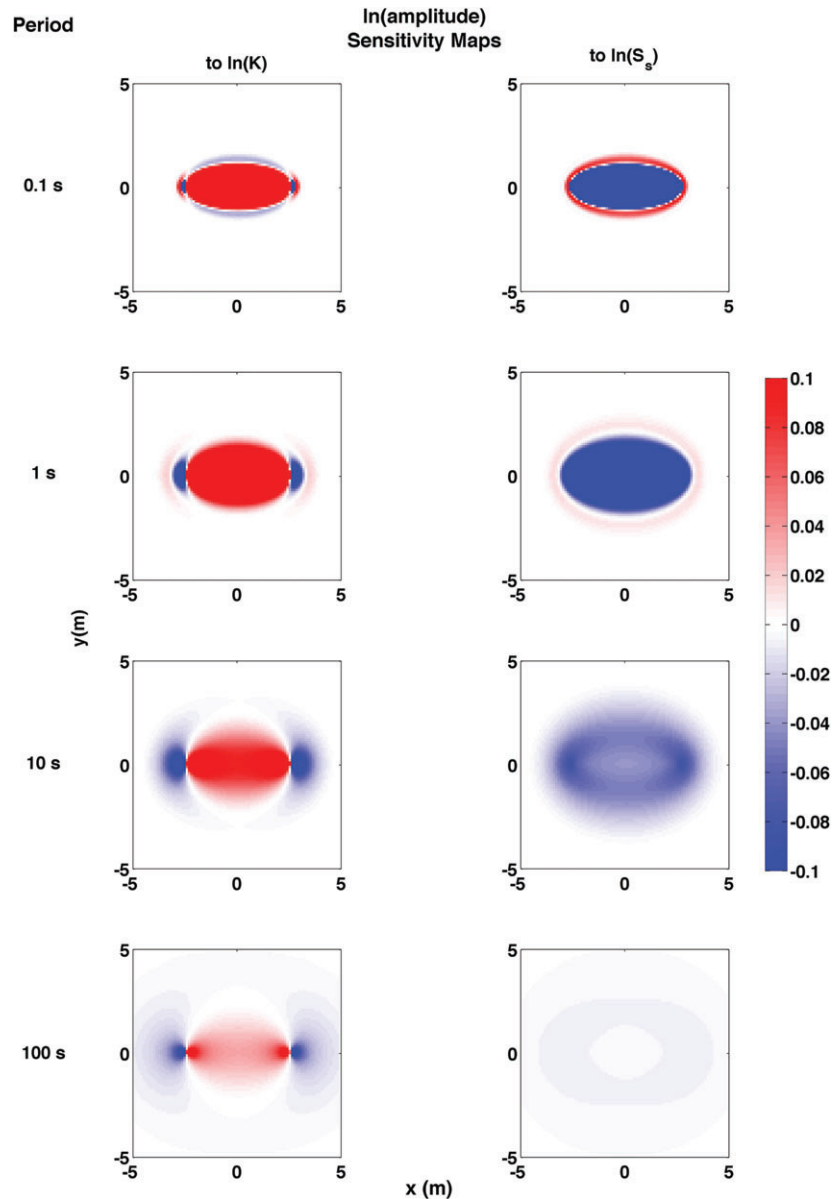


Figure 4. Example of sensitivity maps produced through combination of analytical solution with adjoint theory. Sensitivities are unitless sensitivity of  $\ln(\text{signal amplitude})$  to  $\ln(K)$  and  $\ln(S_s)$ . All maps use the same scale, with red representing positive and blue representing negative sensitivities. Note broadening and diffusion of the sensitivity structure at larger periods.

- Sensitivity of log-amplitude,  $\ln(|\Phi_\omega|)$ , to  $\ln(S_s)$ :  $\text{Re}(i\omega\psi_i S_s \Phi_\omega)$ .
- Sensitivity of phase,  $\arg(\Phi_\omega)$ , to  $\ln(K)$ :  $\text{Im}(K \nabla \Phi_\omega \cdot \nabla \psi_i)$
- Sensitivity of phase,  $\arg(\Phi_\omega)$ , to  $\ln(S_s)$ :  $\text{Im}(i\omega\psi_i S_s \Phi_\omega)$ .

## Example Visualizations

We now present one example of how these computations can be used to assess spatial sensitivity of measurements to aquifer parameters. This example considers an aquifer with diffusivity ( $K/S_s$ ) equal to 1, and with a pair of pumping/observation wells spaced 5 m apart, located at  $(-2.5, 0)$  and  $(2.5, 0)$ , respectively.

In Figure 4, the spatial sensitivity structure of  $\ln(\text{amplitude})$  to aquifer parameters is shown across a range of testing periods. While the shortest testing period of 0.1 s may be physically unreasonable, it emphasizes the message that at very short testing periods, the sensitivity is almost entirely contained between the pumping and observation wells. As longer periods are used, the sensitivity structure broadens and “diffuses” outward, showing that these tests will be sensitive to aquifer parameters over a broader area.

These maps emphasize that oscillatory testing data at different stimulation periods should be interpreted carefully, since data from different periods of testing (if fit using a homogeneous model) may produce different “effective” aquifer parameters. This is simply a manifestation of the different averaging volumes of these tests, and may help to explain the “intrinsic period-dependence” of hydraulic properties observed by both Renner and Messar (2006) and Becker and Guiltinan (2010) in previous analyses.

## Summary and Conclusions

Oscillatory pumping tests are not presently a widely used strategy for aquifer characterization. However, the benefits associated with these tests (such as no net water extraction, and multi-frequency sensitivity to different averaging volumes or scales) may prove useful for contaminated site investigation and other purposes. In this paper, we have developed several analytical tools that can be used to design and analyze oscillatory pumping tests. While the background mathematics for some of these tools is fairly involved—using phase-domain mathematics—all key results can be applied immediately with pencil and paper, or through MATLAB programs using a laptop computer. It is the authors’ hope that these simple tools will make the application of oscillatory pumping tests more approachable, and will produce effective designs for oscillatory testing in the field.

We first presented a set of formulas that can be used to choose appropriate oscillatory pumping test design parameters, given only limited knowledge of bulk or “effective” aquifer properties. Based on the aquifer parameters and a planned machinery design, the

key formulas presented (Equations 18–20 and Equations 24–26) can be used to quickly determine reasonable testing strategies. With significant design constraints, simple MATLAB codes can be used to verify testing feasibility. After using this approach to develop a testing strategy for a field campaign at the BHRS in Boise, ID, we showed how results from the field testing indicate that the testing design parameters used were well-optimized.

Secondly, we presented a method for understanding how the response to an oscillatory pumping test will be dependent on spatially distributed aquifer parameters. The code presented uses analytical solutions for oscillatory tests coupled with an adjoint sensitivity analysis to quickly and analytically derive sensitivity maps. Again, by using only a simple MATLAB program and bulk estimates of aquifer parameters, a field practitioner can understand the spatial volume or scale “covered” by a given oscillatory pumping test, and how this sensitivity changes as a function of the oscillatory testing period.

## Acknowledgments

This work was supported by NSF Awards 1215746 and 1215768, and by ARO URISP award W911NF1110291. Additional computational resources were provided by the UW-Madison Center for High-Throughput Computing (CHTC) and the Advanced Computing Initiative (ACI). Cost share and design input by Mt. Sopris Instruments (especially, James Koerlin) for development of the oscillating signal generator is gratefully acknowledged. The authors thank colleagues David Hochstetler, Tania Bakhos, Peter K. Kitanidis, YaoQuan Zhou, and Michael Thoma, all of whom took part in design and field data collection for the oscillatory pumping test data presented in this work. Finally, the authors thank reviewers Keith J. Halford and Hund-Der Yeh, whose comments greatly contributed to the refinement of this manuscript.

## Supporting Information

Additional Supporting Information may be found in the online version of this article:

**Appendix S1.** Appendix containing a full derivation of the algorithm for determining period/flow rate optima for the case where multiple testing constraints are considered.

**Appendix S2.** A .zip file containing MATLAB codes described in this paper, along with “click to run” supporting codes. Please view the README.TXT within the .zip file for further information.

## References

- Bakhos, T., M. Cardiff, W. Barrash, and P.K. Kitanidis. 2014. Data processing for oscillatory pumping tests. *Journal of Hydrology* 511: 310–319. DOI:10.1016/j.jhydrol.2014.01.007.
- Barrash, W., and T. Clemo. 2002. Hierarchical geostatistics and multifacies systems: Boise Hydrogeophysical Research

- Site, Boise, Idaho. *Water Resources Research* 38, no. 10: 1196.
- Barrash, W., T. Clemo, J.J. Fox, and T. Johnson. 2006. Field, laboratory, and modeling investigation of the skin effect at wells with slotted casing, Boise Hydrogeophysical Research Site. *Journal of Hydrology* 326: 181–198. DOI:10.1016/j.jhydrol.2005.10.029.
- Barrash, W., T. Clemo, and M.D. Knoll. 1999. Boise Hydrogeophysical Research Site (BHRS): Objectives, design, initial geostatistical results. In *Symposium on the Application of Geophysics to Engineering and Environmental Problems (SAGEEP)*. Oakland, California: Environmental and Engineering Geophysical Society.
- Becker, M., and E. Guiltinan. 2010. Cross-hole periodic hydraulic testing of inter-well connectivity. Stanford Geothermal Workshop. Stanford, California: Stanford University.
- Black, J.H., and K.L. Kipp Jr. 1981. Determination of hydrogeological parameters using sinusoidal pressure tests: A theoretical appraisal. *Water Resources Research* 17, no. 3: 686–692. DOI:10.1029/WR017i003p00686.
- Butler, J.J. Jr. 1998. *The Design, Performance, and Analysis of Slug Tests*. Boca Raton, Florida: Lewis Publishers.
- Cardiff, M., and P.K. Kitanidis. 2008. Efficient solution of nonlinear, underdetermined inverse problems with a generalized PDE model. *Computers and Geosciences* 34: 1480–1491. DOI:10.1016/j.cageo.2008.01.013.
- Cardiff, M., T. Bakhos, P.K. Kitanidis, and W. Barrash. 2013a. Aquifer heterogeneity characterization with oscillatory pumping: Sensitivity analysis and imaging potential. *Water Resources Research* 49, no. 9: 5395–5410. DOI:10.1002/wrcr.20356.
- Cardiff, M., W. Barrash, and P.K. Kitanidis. 2013b. Hydraulic conductivity imaging from 3-D transient hydraulic tomography at several pumping/observation densities. *Water Resources Research* 49, no. 11: 7311–7326. DOI:10.1002/wrcr.20519.
- Cardiff, M., W. Barrash, and P.K. Kitanidis. 2012a. A field proof-of-concept of aquifer imaging using 3D transient hydraulic tomography with temporarily-emplaced equipment. *Water Resources Research* 48: W05531. DOI:10.1029/2011WR011704.
- Cardiff, M., W. Barrash, and P.K. Kitanidis. 2012b. Oscillatory hydraulic tomography: Numerical studies. In *Computational Methods in Water Resources (CMWR)*. Champaign, Illinois: University of Illinois at Urbana-Champaign.
- Cardiff, M., W. Barrash, B. Malama, and M. Thoma. 2011. Information content of slug tests for estimating hydraulic properties in realistic, high-conductivity aquifer scenarios. *Journal of Hydrology* 403, no. 1–2: 66–82. DOI:10.1016/j.jhydrol.2011.03.044.
- Cardiff, M., W. Barrash, P.K. Kitanidis, B. Malama, A. Revil, S. Straface, and E. Rizzo. 2009. A potential-based inversion of unconfined steady-state hydraulic tomography. *Ground Water* 47, no. 2: 259–270. DOI:10.1111/j.1745-6584.2008.00541.x.
- Cirpka, O.A., and P.K. Kitanidis. 2001. Sensitivities of temporal moments calculated by the adjoint-state method and joint inverting of head and tracer data. *Advances in Water Resources* 24, no. 1: 89–103.
- Fokker, P.A., J. Renner, and F. Verga. 2013. Numerical modeling of periodic pumping tests in wells penetrating a heterogeneous aquifer. *American Journal of Environmental Sciences* 9: 1–13.
- Hollaender, F., P.S. Hammond, and A. Gringarten. 2002. Harmonic testing for continuous well and reservoir monitoring. Paper SPE 77692 presented at the 2002 SPE Annual Technical Conference and Exhibition, San Antonio, Texas.
- Jazayeri Noushabadi, M.R., H. Jourde, and G. Massonnat. 2011. Influence of the observation scale on permeability estimation at local and regional scales through well tests in a fractured and karstic aquifer (Lez aquifer, Southern France). *Journal of Hydrology* 403, no. 3–4: 321–336. DOI:10.1016/j.jhydrol.2011.04.013.
- Johnson, C.R., R. Greenkorn, and E. Woods. 1966. Pulse-testing: A new method for describing reservoir flow properties between wells. *Journal of Petroleum Technology* 18, no. 12: 1599–1604.
- Kuo, C.H. 1972. Determination of reservoir properties from sinusoidal and multirate flow test in one or more wells. *SPE Journal* 12, no. 6: 499–507.
- Lavenue, M., and G. de Marsily. 2001. Three-dimensional interference test interpretation in a fractured aquifer using the Pilot Point Inverse Method. *Water Resources Research* 37, no. 11: 2659–2675. DOI:10.1029/2000wr000289.
- Leven, C., and P. Dietrich. 2006. What information can we get from pumping tests?—Comparing pumping test configurations using sensitivity coefficients. *Journal of Hydrology* 319: 199–215.
- Maineult, A., E. Strobach, and J. Renner. 2008. Self-potential signals induced by periodic pumping tests. *Journal of Geophysical Research* 113, no. B01203: 12. DOI:10.1029/2007JB005193.
- McElwee, C.D., B.R. Engard, B.J. Wachter, S.A. Lyle, J. Healey, and J.F. Devlin. 2011. Hydraulic tomography and high-resolution slug testing to determine hydraulic conductivity distributions. KGS Open-File Reports (2011-02): 168.
- Neupauer, R.M., and J.L. Wilson. 1999. Adjoint method for obtaining backward-in-time location and travel time probabilities of a conservative groundwater contaminant. *Water Resources Research* 35, no. 11: 3389–3398.
- Rasmussen, T.C., K.G. Haborak, and M.H. Young. 2003. Estimating aquifer hydraulic properties using sinusoidal pumping at the Savannah River site, South Carolina, USA. *Hydrogeology Journal* 11: 466–482. DOI:10.1007/s10040-003-0255-7.
- Renner, J., and M. Messar. 2006. Periodic pumping tests. *Geophysical Journal International* 167: 479–493. DOI:10.1111/j.1365-246X.2006.02984.x.
- Revil, A., C. Gevaudan, N. Lu, and A. Maineult. 2008. Hysteresis of the self-potential response associated with harmonic pumping tests. *Geophysical Research Letters* 35, no. 16: L16402. DOI:10.1029/2008gl035025.
- Rosa, A., and R. Horne. 1997. Reservoir description by well test analysis using cyclic flow rate variation. *SPE Formation Evaluation* 12, no. 4: 247–254.
- Smith, A.J. 2008. Weakly nonlinear approximation of periodic flow in phreatic aquifers. *Ground Water* 46, no. 2: 228–238. DOI:10.1111/j.1745-6584.2007.00418.x.
- Sykes, J.F., J.L. Wilson, and R.W. Andrews. 1985. Sensitivity analysis for steady state groundwater flow using adjoint operators. *Water Resources Research* 21, no. 3: 359–371.
- Townley, L.R. 1993. AQUIFEM-P: A periodic finite element aquifer flow model: User's manual and description. CSIRO Division of Water Resources Technical Memorandum 93/13. 72 pp, plus software.
- Vela, S., and R. McKinley. 1970. How areal heterogeneities affect pulse-test results. *SPE Journal* 10, no. 2: 479–493.
- Yeh, H.-D., and Y.-C. Chang. 2013. Recent advances in modeling of well hydraulics. *Advances in Water Resources* 51: 27–51. DOI:10.1016/j.advwatres.2012.03.006.